Chemical Engineering Journal 162 (2010) 296–300

Contents lists available at ScienceDirect

Chemical Engineering Journal

journal homepage: www.elsevier.com/locate/cej

Identification of regime transitions in an inner-loop airlift reactor using local bubble-induced pressure fluctuation signals

Wen-Hui Zhang[a,b], Hong Li[b], Xingang Li[b,*]

[a] Tianjin Key Lab of Pulp and Paper, College of Material Science & Chemical Engineering, Tianjin University of Science & Technology, Tianjin 300457, China
[b] Department of Chemical Engineering, School of Chemical Engineering and Technology, Tianjin University, 92 Weijin Road, Nankai District, Tianjin 300072, China

ARTICLE INFO

Article history:
Received 17 January 2010
Received in revised form 17 April 2010
Accepted 20 April 2010

Keywords:
Pressure fluctuation signals
Local energy ratio
Correlation dimension
Kolmogorov entropy
Flow regime

ABSTRACT

The local bubble-induced pressure fluctuation signals, which were extracted by Zhang's method [15], were used to identify the flow regime in an inner-loop airlift reactor. For this purpose, local energy ratio and chaotic analysis were employed to extract useful information in detecting the flow regime transition. It was found that local energy ratio was able to indicate the two transition points in the downcomer and two transition points in the riser. Correlation dimension and Kolmogorov entropy can also detect two transition points in the downcomer, but only one transition points in the riser. Since the local energy ratio was easy to calculate, it had a great potential for detecting flow regime transition in an internal-loop airlift reactor or other multiphase systems.

1. Introduction

Internal-loop airlift reactors (ILALR) have been found useful in the bio-processing and wastewater treatment industry due to low power consumption, low maintenance costs, low shear stress and sufficient oxygen transfer rate [1]. It is a type of multiphase contactor consisting of two concentric cylinders with a gas distributor at the bottom and a separator at the top. In the riser or drat tube, the homogeneous regime occurs at low superficial gas velocity, and may turn into the transition regime with an increase of superficial gas velocity and enters the heterogeneous regime at high superficial gas velocity. In the downcomer, there are mainly three different flow regimes: regime I, which corresponds to no gas entrainment in the downcomer; regime II, which corresponds to gas entrainment without gas recirculation in the downcomer; regime III, which gas recirculation is completed in the downcomer [2,3]. The transition could be instantaneous or expanded transition, which has been influenced by many factors, such as column geometry, sparger design and operation conditions. The study of flow transition is important for improvement of design, operation and control of the reactor. However, the determination of flow transition or flow regime is not easy due to complicated mechanisms.

Since the measurement of pressure fluctuation signals is relatively cheap and well developed, it has a great potential application in experimental condition and industrial conditions. In recent years, most of the studies on flow transition in the gas–liquid systems have been focused on the wall pressure fluctuation signals or differential pressure fluctuation signals. Meanwhile, several analysis methods are successfully applied to extract useful information from pressure fluctuation signals for flow regime detection [3–15]. In the early years, statistical analysis was mainly adopted in detecting flow regime. Fan et al. [4] have attempted to characterize the flow regimes in a gas–liquid–solid fluidized bed by the statistical properties of the wall pressure fluctuations signals, specifically the power spectral density function and the root mean square of the pressure fluctuations signals. More recently, many advanced analysis methods were applied in detecting flow transition. Many researchers have found that [5–11] chaotic analysis of pressure fluctuation signal could be a powerful technique for identification of flow regimes in multiphase reactor. Ruthiya et al. [12] have employed the coherent standard deviation and the average frequency of wall pressure fluctuation signals to determine flow regimes in a slurry bubble column. Briens and Ellis [13] have applied statistical, fractal, chaos and wavelet analysis methods to examine the hydrodynamics of three-phase fluidized bed systems and found that the standard deviations of the decomposed signals through wavelet transformation could be successfully in flow regime detection. Al-Masry et al. [14] have applied auto-correlation function on the differential pressure fluctuation signals in determining flow regime transition.

Since the hydrodynamics of multiphase reactor has relation with bubble characteristics, it may be a better way to apply bubble-induced pressure fluctuation signals directly in flow regime detection. In the most recent year, Zhang et al. [15] have studied

* Corresponding author. Tel.: +86 022 27404701; fax: +86 022 27404705.
E-mail address: lxg@tju.edu.cn (X. Li).

1385-8947/$ – see front matter
doi:10.1016/j.cej.2010.04.038

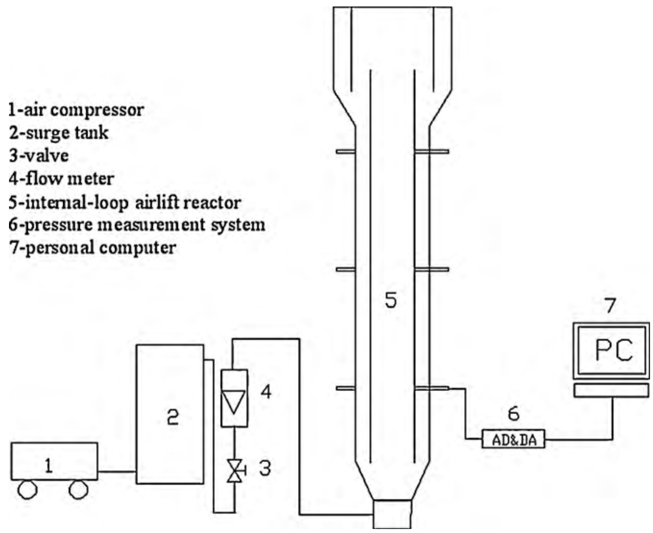

Fig. 1. The schematic diagram of the experiment.

the origin of wall pressure fluctuation signals in an internal-loop airlift reactor and found that the bubble-induced pressure fluctuation signals could be extracted by wavelet and coherence analysis method. Hence, the aim of this paper is to adopt Zhang's method to extract local bubble-induced pressure fluctuation signals from wall pressure fluctuation signals and apply local energy ratio and chaotic analysis of them in determining the flow regime transitions in the reactor.

2. Equipment and experimental methods

The schematic diagram of the experiment was shown in Fig. 1. The reactor was constructed of 0.186 m ID Plexiglas column and 1.5 m in height. The inside diameter of the draft tube was 0.11 m and the height was 1.02 m; the draft tube was located 0.08 m above the gas distributor. The inside diameter of the enlarged section at top column was 0.28 m; the inside diameter of the separator tube was 0.186 m; the top clearance (the distance between the liquid surface and the upper end of the draft tube) was 0.1 m. The gas distributor was a perforated plate containing 64 holes of 0.8 mm diameter arranged in an equilateral triangular configuration. The gas was oil-free air and the liquid was tap water maintained at $293 \pm 0.5k$. All experiments were operated at superficial gas velocity between 1.46 and 11.7 cm/s (based on draft tube area).

High dynamic pressure transducers were used to measure wall pressure fluctuation signals within the reactor. The sampling ports were located at 0.33, 0.59, 0.98 m height above gas distributor in the riser and in the downcomer. All signals were sampled by a data acquisition system (PCI 6220 board, LABVIEW 8.0 data acquisition software) at a frequency of 400 Hz for intervals of 300 s.

3. Analysis methods

3.1. Wavelet transform

Wavelet transform is a newly developed time frequency analysis method that has been shown to be a powerful tool for revealing local signal characteristics such as local turbulence or local bubble characteristic [15,16].

The discrete wavelet transform allows the decomposition of signals into different resolution components. Each level of decomposition contains information associated with a scale, which can be related to the pseudo-frequency by associating a purely periodic signal of frequency with a given wavelet. After decomposition, high-scale and low frequency components of the signal are called approximations (*As*), and low-scale and high-frequency components of the signal are called details (*Ds*). For discrete wavelet transform, the discrete wavelet coefficients W_{ij} at dyadic scale j and displacement k can be expressed as

$$W_{jk} = \frac{1}{\sqrt{N}} \sum x(i)\psi_{jk}(i)$$

where $\{x(i)\}$ is time series data whose length is N. The wavelet function $\psi_{ij}(i)$ can be expressed as

$$\psi_{jk}(i) = 2^{j/2}\psi(2^j i - k)$$

where $j = 0, 1, ..., J$ and $k = 1, ..., 2^J$ with $J = \log N/\log 2$.

Daubechies wavelet is often used for signal decomposition due to its higher number of vanishing moments for a given support width. In this study, Daubechies 12th order wavelet is applied in wall pressure fluctuation signal decomposition, which is selected on minimizing the upper bound on the 2-norm of the signal approximation error at the desired resolution level [17].

3.2. Deterministic chaotic analysis

A chaotic system is a non-linear, deterministic system that exhibits a great sensitivity to small modifications in initial condition [18]. So far, the chaotic phenomenon has been found to prevail in multiphase systems such as gas–solid, gas–liquid or gas–liquid–solid systems [5,7,8,10,11]. The correlation dimension ($D2$) and the Kolmogorov entropy ($K2$) are two important chaotic invariants, which have been shown to be useful in predicting hydrodynamics of multiphase systems.

$D2$ can be determined from the relation as follows [19]:

$$\lim_{\substack{r \to 0 \\ N \to \infty}} C_m(r, N)) \propto r^{D2}$$

where r is the distance between two point in the phase space, m is embedding dimension. The correlation integral, $C_m(r, N)$ is defined as

$$C_m(r, N) = \lim_{n \to \infty} \frac{1}{N^2} \Sigma H(r - ||X_i(m, \tau) - X_j(m, r)||)$$

where X_i is the m-dimensional reconstructive vector drawn from the time series of wall pressure fluctuation signals, x_i with time delay τ. N is the length of time series of wall pressure fluctuation signals

$$X_i = \{x_i, x_{i+\tau}, \ldots, x_{i+(m-1)\tau}\}, \quad (i = 1, 2, \ldots, N)$$

$K2$ can be estimated as follows [20]:

$$K2 \propto \lim_{m \to \infty} \lim_{r \to 0} K_{2,m}(r, N)$$

where $K_{2,m}(r, N)$ is defined as

$$K_{2,m}(r, N) = \frac{1}{\tau} \ln \frac{C_m(r)}{C_{m+1}(r)}$$

Time delay and embedding dimension can be determined by the mutual information method [21] and Cao's method [22] respectively.

4. Results and discussion

4.1. Pre-treatment of wall pressure fluctuation by wavelet analysis

Pressure fluctuations in multiphase system are of multi-scale and complex in nature [23]. Wall pressure fluctuations could be

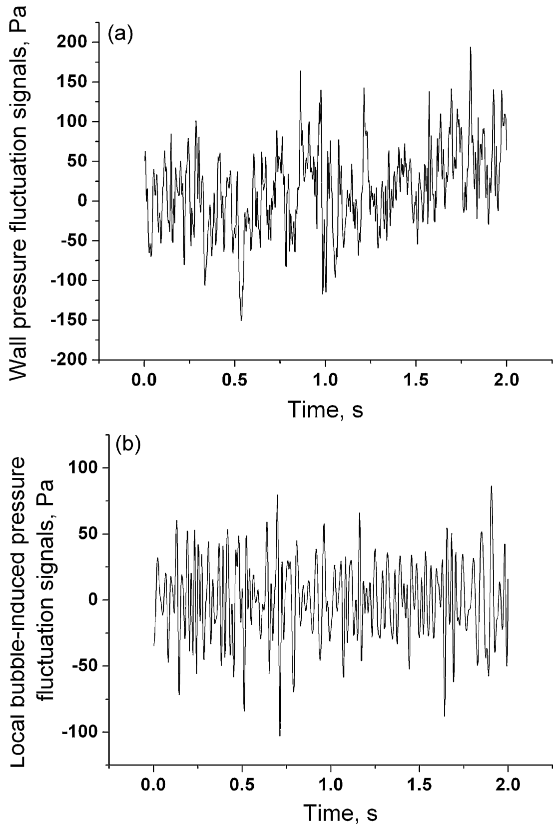

Fig. 2. The typical wall pressure fluctuation signals (a) and local bubble-induced pressure fluctuation signals (b).

classified into two types: global pressure fluctuations, which are mainly generated by air supply system, bubble eruption at surface bed, etc. and local pressure fluctuations, which are mainly caused by bubble movement, breakup and liquid vortex, etc. [15,24,25].

Since the flow regime transition is associated with local bubble-induced pressure fluctuation signals, this paper adopt Zhang's method to extract local bubble-induced pressure fluctuation signals from wall pressure fluctuation signals. The pre-treatment method was as follows:

(a) Decompose origin wall pressure fluctuation signals into different resolution components by Daubechies 12th order wavelet.
(b) Calculate the coherence of two wall pressure fluctuation signals.
(c) Determine the details (*Ds*) with low coherence, which is less than a certain value (such as 0.75).
(d) Add all the details with low coherence except for the details influenced obviously by noise.

After wall pressure fluctuation signals have been pre-treated as above, the local bubble-induced pressure fluctuation signals, which could be expressed by $Ds3 + Ds4$ (or a linear superposition of $Ds3$ and $Ds4$) in this works, were obtained. The typical wall pressure fluctuation signals and local bubble-induced pressure fluctuation signals are shown in Fig. 2.

4.2. Correlation dimension and Kolmogorov entropy

Firstly, in order to understand the regimes occurred in the reactor, visual observations in the internal-loop airlift reactor were described as follow: in the downcomer, at the lowest superficial gas velocity, liquid recirculation velocity was too low to carry bubbles into the downcomer, which corresponds to regime I. With the increase of superficial gas velocity, bubbles began to enter the downcomer without recirculation, which corresponds to regime II. Then, as the velocity increases further, small bubbles began to flow downwards and into the riser, which corresponds to regime III-1; at higher superficial gas velocity, bigger bubbles began recirculation, which corresponds to regime III-2. In the riser, at low superficial gas velocity, bubble size almost did not vary with superficial gas velocity, which corresponds to homogenous regime; at high superficial gas velocity, bubble size became large and the distribution of bubble size becomes broader, which corresponds to heterogeneous regime.

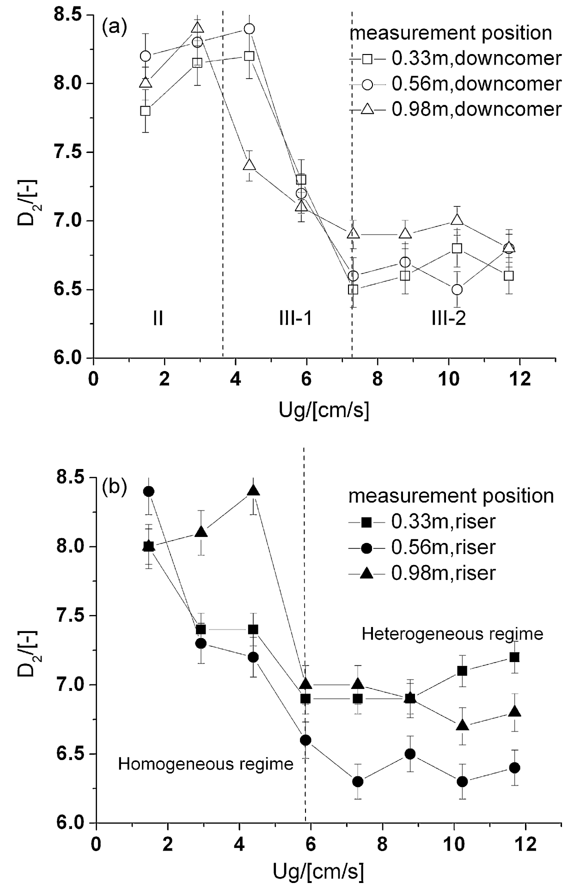

Fig. 3. *D*2 of bubble-induced pressure fluctuation signals in the downcomer (a) and in the riser (b) respectively at different superficial gas velocities.

According to gas holdup data (which was shown in another paper [15]), we can find three flow regimes (regime I, regime III-1 and regime III-2) in the downcomer and two flow regimes (homogeneous regime and heterogeneous regime) in the riser, which was similar with van Benthum's result [3]. However, it cannot indicate regime II in the downcomer and the transition flow regime in the riser.

In order to determine the regime transition, two chaotic invariants of bubble-induced pressure fluctuation signals were investigated. The length of data was 40,000. The embedding dimension was 14 estimated by Cao's method at all the superficial gas velocity and the time delay was different estimated by mutual information method at all the supercritical gas velocity.

The correlation dimension (*D*2) of a chaotic system could indicate the complex of the system. Fig. 3a and b shows that *D*2 of bubble-induced pressure fluctuation signals in the downcomer and in the riser respectively varies with different superficial gas velocity. In Fig. 3a, it is shown that the general trend of *D*2 first increases slightly across first transition point (corresponding to the transition between regime II and regime III-1), then decreases rapidly across second transition point (corresponding to regime III-1 and regime III-2) and changes with gas velocity at high superficial gas velocity. In Fig. 3b, it is shown that the trend of $D2$ in the riser decreases with superficial gas velocity at low gas velocity and almost does not change with gas velocity at high gas velocity, except for the highest measurement position.

In the downcomer, the number of bubble increases with superficial gas velocity in regime II, which leads to the increase of the complex of system. Above the first transition point, the system enters regime III-1, bubbles move more regularly due to high liquid circulation velocity and the complex of system decreased fast, which is similar to the phenomenon of “self-organization” [5]. As gas velocity increases further and across the second transition point, the complex of system reaches a steady state due to bigger bubble movement and “self-organization” phenomenon. In the riser, small bubbles rise through the column in a straight line at low superficial gas velocity, almost all the bubbles has approximately the same speed. As superficial gas velocity increases (in the homogenous regime), the liquid recirculation velocity also increases, which leads to bubble movement more regularly and the complex of system decreases fast. However, at the highest measurement position, bubble movement is not the same as the other measurement positions within reactor due to significant change of bubble velocity direction, which may decreases the complex of system much slowly at low superficial gas velocity. After the transition point, the flow enters the heterogeneous regime and the complex of system reaches a steady state due to bigger bubble movement or breakup and “self-organization” phenomenon.

Kolmogorov entropy can be thought of a number measuring the time rate of creation of information or information loss rate as a chaotic obit evolves. Fig. 4a and b shows that $K2$ of local bubble-induced pressure fluctuation signals in the downcomer and in the riser respectively varies with different superficial gas velocity. The change trends of $K2$ is almost the same as the one of $D2$, which is similar with the results of Karamavruq et al. [26]. It is because that more or bigger bubble movement leads to the increase of information loss rate and “self-organization” phenomenon leads to the decrease of information loss rate.

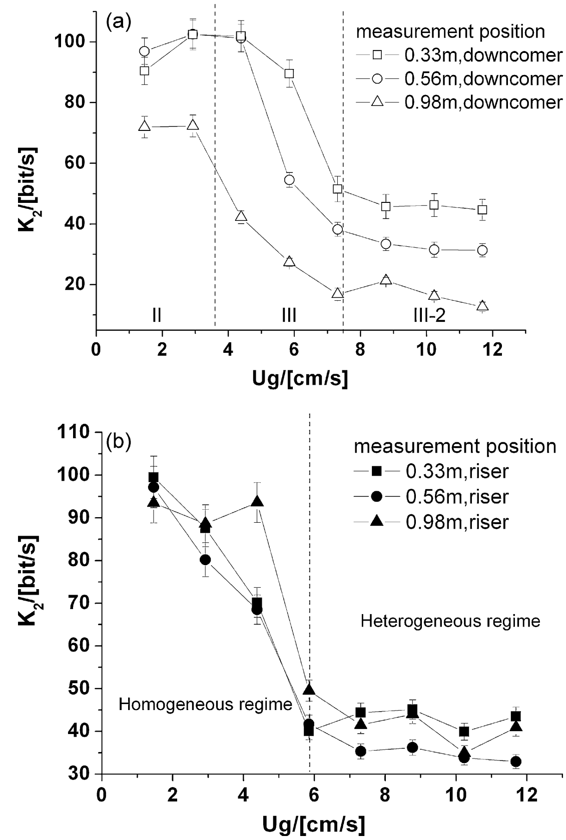

Fig. 4. $K2$ of local bubble-induced pressure fluctuation signals in the downcomer (a) and in the riser (b) respectively at different superficial gas velocities.

4.3. Local energy ratio

Since the local bubble-induced pressure fluctuation signals could be associated with bubble size, bubble movement and breakup [15,25], the energy of local bubble-induced pressure fluctuation may have different variation tendency in different flow regimes. Here, we use the local energy ratio, defined as the ratio between the energy of local bubble-induced pressure fluctuation signals and the energy of wall pressure fluctuation signals, to detect flow regime transition. It can be expressed as follows:

$$\zeta_L = \frac{E_{Local}}{E_{Total}} = \left(\frac{\sigma_{Local}}{\sigma}\right)^2$$

where σ_{Local} and σ are the standard deviation of local bubble-induced pressure fluctuation signals and wall pressure fluctuation signals respectively.

Fig. 5a and b show that the local energy ratio of pressure fluctuation signals in the downcomer and in the riser respectively varies with superficial gas velocity. In Fig. 5a, it is shown that in the downcomer, the general trend of the local energy ratio first increases fast across the first transition point (corresponding to the transition between regime II and regime III-1), then increases moderately with gas velocity across the second transition point (corresponding to the transition between regime III-1 and regime III-2) and

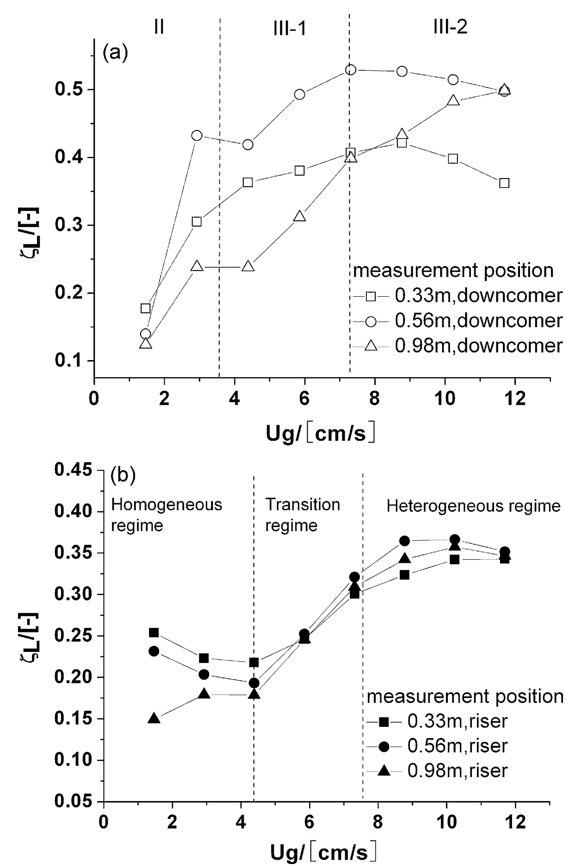

Fig. 5. Local energy ratio of pressure fluctuation signals in the downcomer (a) and in the riser (b) respectively at different superficial gas velocities.

decreases or increases slowly at high superficial gas velocity. In Fig. 5b, it is shown that in the riser, the general trend of the local energy ratio first decreases slightly across the first transition point except for the highest measurement position (corresponding to the transition between homogeneous regime and transition regime), then increases fast with gas velocity across the second transition point (corresponding to the transition between transition regime and heterogeneous regime) and almost does not change with gas velocity at high superficial gas velocity.

In the riser, when the superficial gas velocity is below the first transition point, the energy of local bubble-induced pressure fluctuation increases with gas velocity mainly due to the increase of bubble number instead of bubble size. Since the energy of global pressure fluctuation increases fast due to gas supply system and attenuates along the axial direction [15], it leads to the decrease of local energy ratio at lower measurement positions and the slight increase of local energy ratio at the highest measurement position. After gas velocity is above the first transition point, the flow enters the transition regime. Local energy ratio increases with gas velocity mainly due to the increase of not only bubble number but also bubble size. After gas velocity is above the second transition point, the energy of global pressure fluctuation due to gas supply system and the energy of local bubble-induced pressure fluctuation caused by bubble movement, coalescence and breakage increases almost at the same rate; hence local energy ratio almost does not change.

In the downcomer, the second transition point can be explained by the same reason as the one in the riser; the first transition point can be explained by two reasons: one is that the increase of bubble number will increase the energy of local bubble-induced pressure fluctuation and the other is that the turn-back flow zone between the riser and the downcomer leads to the attenuation of global pressure fluctuation at low superficial gas velocity.

As a conclusion, the increase rate of local-energy ratio has a relation with the regime hydrodynamic in the reactor, which indicates the flow transition.

5. Conclusions

In this paper, the flow regimes and their transition points in an internal-loop airlift reactor were studied. Flow regime transitions were predicted by local energy ratio and chaotic analysis in the local bubble-induced pressure fluctuation signals, which can be extracted by Zhang's method from wall pressure fluctuation signals.

As far as local energy ratio analysis method was concerned, it was found that local energy ratio can indicate four transition points in the reactor, including the first transition point (around 4.38 cm/s) from regime II and to III-1 in the downcomer, the second transition point (around 7.31 cm/s) from regime III-1 to regime III-2 in the downcomer, the first transition point (around 4.38 cm/s) from homogeneous regime to transition regime in the riser, and the second transition point (around 8.77 cm/s) from transition regime to heterogeneous regime in the riser respectively. The two transition points in the riser were similar with the ones predicted by Lin et al. [8] in a bubble column.

For chaotic analysis method, two chaotic invariants including correlation dimension and Kolmogorov entropy can detect two transition points in the downcomer, which were almost the same as that indicated by local energy ratio analysis. However, the two chaotic parameters can detect only one transition point (around 5.81 cm/s) from homogenous regime to heterogeneous regime.

It should be noted that local energy ratio and chaotic analysis methods were able to determine the flow regime transition in the reactor. Since the local energy ratio analysis method was easy to implement, it can be a novel method to detect flow regime transition in internal-loop airlift reactors or other multiphase systems.

Acknowledgement

The authors gratefully acknowledge the financial supports by Startup Funding for New Faculty of Tianjin University Science & Technology (No. 20090419).

References

[1] M.Y. Chisti, Airlift Bioreactors, Elsevier Applied Science, New York, 1989.
[2] J.J. Heijnen, J. Hols, R.G.J.M. van der Lans, H.L.J.M. van Leeuwen, A. Mulder, R. Weltevrede, A simple hydrodynamic model for the liquid circulation velocity in a full-scale two- and three-phase internal airlift reactor operating in the gas recirculation regime, Chem. Eng. Sci. 52 (1997) 2527–2540.
[3] W.A.J. van Benthum, R.G.J.M. van der Lans, M.C.M. van Loosdrecht, J.J. Heijnen, Bubble recirculation regimes in an internal-loop airlift reactor, Chem. Eng. Sci. 54 (1999) 3995–4006.
[4] L.-S. Fan, S. Satija, K. Wisecarver, Pressure fluctuation measurements and flow regime transitions in gas–liquid–solid fluidized beds, AIChE J. 32 (1986) 338–340.
[5] H.M. Letzel, J.C. Schouten, R. Krishna, C.M. van den Bleek, Characterization of regimes and regime transitions in bubble columns by chaos analysis of pressure signals, Chem. Eng. Sci. 52 (1997) 4447–4459.
[6] V.R. Ranade, V.P. Utikar, Dynamics of gas–liquid flows in bubble column reactors, Chem. Eng. Sci. 54 (1999) 5237–5243.
[7] D. Bai, A.S. Issangya, J.R. Grace, Characteristics of gas-fluidized beds in different flow regimes, Ind. Eng. Chem. Res. 38 (1999) 803–811.
[8] T.-J. Lin, R.-C. Juang, Y.-C. Chen, C.-C. Chen, Predictions of flow transitions in a bubble column by chaotic time series analysis of pressure fluctuation signals, Chem. Eng. Sci. 56 (2001) 1057–1065.
[9] B. Gourich, C. Vial, A.H. Essadki, F. Allam, M.B. Soulami, M. Ziyad, Identification of flow regimes and transition points in a bubble column through analysis of differential pressure signal—influence of the coalescence behavior of the liquid phase, Chem. Eng. Process. 45 (2006) 214–223.
[10] L.-S. Hu, X.-J. Wang, G.-S. Yu, Y.F. Wang, Z.J. Zhou, F.-C. Wang, Z.-H. Yu, Chaotic analysis of pressure fluctuation signal in the gas–liquid–solid slurry column, Nonlinear Anal. Real World Appl. 10 (2009) 410–415.
[11] C.-C. Fu, L.-S. Fan, W.-T. Wu, Flow regime transitions in an internal-loop airlift reactor, Chem. Eng. Tech. 30 (2007) 1077–1082.
[12] K.C. Ruthiya, V.P. Chilekar, M.J.F. Warnier, J. van der Schaaf, B.F.M. Kuster, J.C. Schouten, J.R. van Ommen, Detecting regime transitions in slurry bubble columns using pressure time series, AIChE J. 51 (2005) 1951–1965.
[13] L.A. Briens, N. Ellis, Hydrodynamics of three-phase fluidized bed systems examined by statistical, fractal, chaos and wavelet analysis methods, Chem. Eng. Sci. 60 (2005) 6094–6106.
[14] W.A. Al-Masry, E.M. Ali, N.N. Al-Kalbani, Prediction of regime transitions in bubble columns using acoustic and differential pressure signals, Chem. Eng. J. 133 (2007) 139–149.
[15] W. Zhang, X. Li, Origin of pressure fluctuations in an internal-loop airlift reactor and its application in flow regime detection, Chem. Eng. Sci. 64 (2009) 1009–1018.
[16] I. Daubechies, Ten Lectures on Wavelets, Society for Industrial and Applied Mathematics, Philadelphia, 1992.
[17] A.H. Tewfik, D. Sinha, P. Jorgensen, On the optimal choice of a wavelet for signal representation, IEEE T. Inform. Theory 38 (1992) 747–765.
[18] C.M. van den Bleek, J.C. Schouten, Deterministic chaos: a new tool in fluidized bed design and operation, Chem. Eng. J. Biochem. Eng. J. 53 (1993) 75–87.
[19] J. Theiler, Spurious dimension from correlation algorithms applied to limited time-series data, Phys. Rev. A 34 (1986) 2427–2432.
[20] P. Grassberger, I. Procaccia, Estimation of the Kolmogorov entropy from a chaotic signal, Phys. Rev. A 28 (1983) 2591–2593.
[21] A.M. Fraser, H.L. Swinney, Independent coordinates for strange attractors from mutual information, Phys. Rev. A 33 (1986) 1134–1140.
[22] L. Cao, Practical method for determining the minimum embedding dimension of a scalar time series, Physica D 110 (1997) 43–50.
[23] H.T. Bi, A critical review of the complex pressure fluctuation phenomenon in gas–solids fluidized beds, Chem. Eng. Sci. 62 (2007) 3473–3493.
[24] J. van der Schaaf, J.C. Schouten, C.M. van den Bleek, Origin, propagation and attenuation of pressure waves in gas–solid fluidized beds, Powder Technol. 95 (1998) 220–233.
[25] J. van der Schaaf, J.C. Schouten, F. Johnsson, C.M. van den Bleek, Non-intrusive determination of bubble and slug length scales in fluidized beds by decomposition of the power spectral density of pressure time series, Int. J. Multiphas. Flow 28 (2002) 865–880.
[26] A.I. Karamavruq, N.N. Clark, Local differential pressure analysis in a slugging bed using deterministic chaos theory, Chem. Eng. Sci. 52 (1997) 357–370.